

The putative pulsar-wind nebulae of the three Musketeers PSR B1055-52, B0656+14 and Geminga revisited

W. Becker¹, N. Kawai², W. Brinkmann¹, and R. Mignani³

¹ Max-Planck-Institut für extraterrestrische Physik, D-85740 Garching bei München, Germany

² Cosmic Radiation Laboratory, RIKEN, 2-1 Hirosawa, Wako-shi, Saitama 351-01, Japan

³ ESA-STECF, D-85740 Garching bei München, Germany

Received: May 20, 1999 / Accepted: Aug 25 1999

Abstract. We report on the analysis of archival ASCA, ROSAT and BeppoSAX data of PSR B1055-52, PSR B0656+14 and Geminga, performed in order to investigate the reality of the putative $\sim 10 - 20$ arcmin wide X-ray pulsar-wind nebulae recently proposed to exist around these pulsars. In all these cases, the ROSAT and/or BeppoSAX data show that the diffuse and clumpy X-ray nebulae found by ASCA can be resolved in the contribution of unidentified point sources, unlikely related to the pulsars.

Key words: Pulsars: individual (PSR B1055-52, PSR B0656+14, Geminga) – X-rays: general – Stars: neutron

1. Introduction

Rotation-powered pulsars are rapidly spinning and strongly magnetized neutron stars which are radiating at the expense of their rotational energy. This interpretation, first expressed by Pacini (1967) few months before the discovery of radio pulsars, is the basic message of the magnetic braking model. The model predicts that the radiative energy loss of a magnetic dipole, corotating with a neutron star at a period P and period derivative \dot{P} , corresponds to a decrease of the neutron star's rotational energy $\dot{E} \propto P^{-3}\dot{P}$. Although the magnetic braking model in its general meaning is widely accepted, the *observed* spin-modulated emission, which gave pulsars their name, is found to account only for a small fraction of \dot{E} . Efficiencies $\eta = L/\dot{E}$ observed in the radio and optical bands are typically in the range $\sim 10^{-7} - 10^{-5}$ whereas at X- and gamma-ray energies they are about $10^{-4} - 10^{-3}$ and $\sim 10^{-2} - 10^{-1}$, respectively. It is therefore a long standing question how rotation-powered pulsars lose the bulk of their rotational energy.

That the energy loss of rotation-powered pulsars can not be fully accounted for by dipole radiation is known from investigation of the pulsars' braking index $n = 2 - P\ddot{P}/\dot{P}^2$. Pure dipole radiation would imply a braking index $n = 3$, whereas the values observed so far are $n = 2.515 \pm 0.005$ for the Crab

(Lyne et al. 1988), $n = 2.8 \pm 0.2$ for PSR B1509-58 (Kaspi et al. 1994), $n = 2.28 \pm 0.02$ for PSR B0540-69 (Boyd et al. 1995) and $n = 1.4 \pm 0.2$ for the Vela Pulsar (Lyne et al. 1996). The deviation from $n = 3$ is usually taken as evidence that a significant fraction of the pulsar's rotational energy is carried off by a pulsar wind i.e. a mixture of charged particles and electromagnetic fields, which, if the conditions are appropriate, forms a pulsar-wind nebula observable at optical, radio- and X-ray energies.

Such pulsar-wind nebulae (often called plerions or synchrotron nebulae) are known so far *only* for few young and powerful (high \dot{E}) rotation-powered pulsars and for some center-filled supernova remnants, in which a young neutron star is expected but only emission from its plerion is detected. The physical details of how the pulsar-wind is generated and how it interacts with the ambient medium is only poorly understood.

The existence of X-ray bright pulsar-wind nebulae as a common feature surrounding rotation-powered pulsars was recently reported on the basis of ASCA observations (Kawai & Tamura 1996). Indeed, the ASCA data of PSR B1055-52, B0656+14, and Geminga (as well as of several other pulsars) show a faint diffuse and somewhat clumpy emission on scales of $\sim 10 - 20$ arcmin around these objects, which has been interpreted as a result of the interaction between the pulsar wind outflow and the surrounding interstellar matter (Kawai et al. 1998a, 1998b; Shibata et al. 1997).

In this paper, we report on a joint analysis of the archival ASCA and ROSAT data of the fields surrounding PSR B1055-52, B0656+14, and Geminga. The aim of the analysis was to search for soft X-ray emission from the putative ASCA detected pulsar-wind nebulae and to check the possible presence of X-ray point sources in the pulsars' neighborhood, which – due to the wide ASCA point-spread function of ($\simeq 3$ arcmin FWHM) – could result in patterns of diffuse emission and knots. For PSR B1055-52 we additionally made use of X-ray data taken by the Narrow Field Instruments (NFI) aboard BeppoSAX. The objects were selected according to the similarity in their spin-parameters and X-ray emission characteristics (*the three musketeers*, see Becker & Trümper 1997). They are furthermore the only sources with ASCA detected pulsar-wind

nebulae for which sufficiently deep ROSAT and/or BeppoSAX data exist.

2. Data analysis and results

2.1. PSR B1055–52

The 197 ms pulsar PSR 1055–52 is a middle aged neutron star ($\tau = P/2\dot{P} = 5.3 \times 10^5$ yr) with a magnetic dipole component $B_{\perp} = 10^{12}$ G and a spin-down energy of $\log \dot{E} = 34.48$ erg/s. X-ray emission from the pulsar was first detected by Chen & Helfand (1983) using the *Einstein* Observatory and subsequently by *EXOSAT* (Brinkmann & Ögelman 1987) and ROSAT (Ögelman & Finley 1993). The ROSAT data provided enough information to detect for the first time the X-ray pulses and to discriminate between different X-ray emission mechanisms (Ögelman & Finley 1993 and Becker & Trümper 1997 for a summary).

ASCA observations of PSR B1055–52 were performed in January 1995 with the Gas Imaging Spectrometers (GIS) and Solid state Imaging Spectrometers (SIS) detectors for an exposure time of 37 ksec and 34 ksec, respectively. Results on a combined spectral analysis of the pulsar X-ray emission based on ROSAT and ASCA data have been reported by Greiveldinger et al. (1996). Wang et al. (1998) confirmed later on that the ASCA data beyond 1 keV are best fitted by a power-law spectrum, associated with non-thermal emission from the pulsar’s inner magnetosphere.

The detection of a putative pulsar-wind nebula surrounding PSR B1055–52 was communicated by Shibata et al. (1997). Fig. 1 shows a contour plot of the ASCA GIS (unit 2+3) full field of view, showing the position of PSR B1055–52 and its surroundings (gray shaded). The pulsar as well as two sources C1 and C2 are indicated. C1 and C2 were interpreted by Shibata et al. (1997) as “clumps” of X-ray emission caused by an interaction of a pulsar-wind outflow with the local interstellar environment. The very low signal-to-noise ratio of the “clumps” limits the spectral analysis, resulting in large uncertainties in the best-fit parameters and making it impossible to discriminate between different emission models like, e.g., a Raymond-Smith thermal plasma or a power-law (see Table 1 and 2 of Shibata et al. 1997 for details), which is expected in case of plerionic emission.

In order to cross-check the ASCA results on PSR B1055–52 and its surroundings, we have made use of data taken by the Narrow Field Instruments (NFI) aboard BeppoSAX. Of particular interest are the data taken with the Medium Energy Concentrator (MECS), which provides a slightly better angular resolution¹ than the ASCA GIS, whereas both instruments cover a similar energy range. MECS (unit 1-3) has observed the pulsar on 28–29th December 1996 for an effective exposure time of ~ 56 ksec. The Low Energy Concentrator (LECS), which has an observing efficiency of only $\sim 40\%$, provides good data for about 22 ksec. Due to its low

¹ The MECS on-axis point-spread function has a half energy width of about 1.7 arcmin at 1.5 keV.

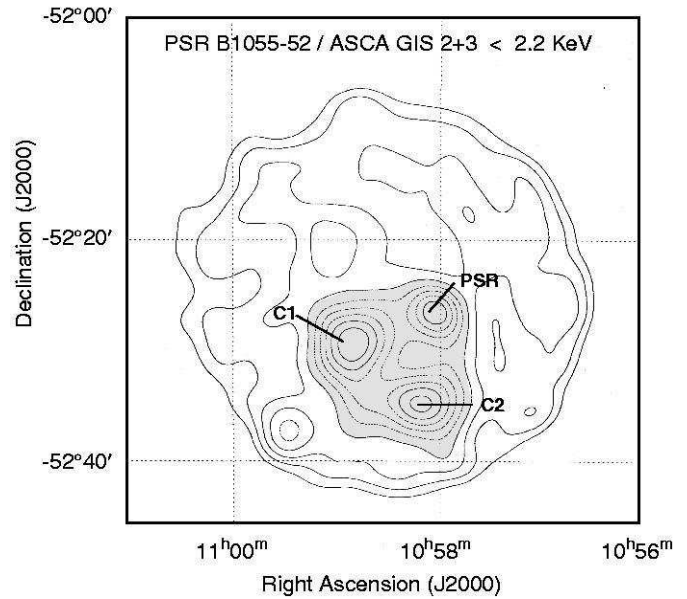


Fig. 1. Contour plot of the region around PSR B1055–52 as seen with the ASCA GIS(2+3). Shown is the GIS full field of view for photon energies below 2.2 keV. The image has been smoothed with a Gaussian filter to increase the visibility of faint emission. The gray-shaded area indicates the emission which is proposed to be from a pulsar-wind nebula (Shibata et al. 1997).

energy response and the soft spectrum of the pulsar’s X-ray emission the LECS provides better data from PSR 1055–52 than the MECS, but doesn’t contribute information on the hard sources C1 and C2.

The MECS image of PSR B1055–52 and its surrounding is given in Fig. 2. As shown, the X-ray sources C1 and C2 neighboring PSR 1055–52 are clearly detected by the MECS, but appear spatially better separated from the pulsar than in the ASCA GIS data. No diffuse and extended component associated with C1 and C2 is detected. Source C2 is found to have a fine structure, clearly visible in Fig. 2 and similarly seen in the ASCA SIS data by Shibata et al. (1997). In addition to C1, C2 and the pulsar, a new source (labeled C4), visible in the north-western edge of Fig. 2, has been detected.

The properties of the MECS detected sources are summarized in Table 1. Since spectral fitting of these sources is precluded by the low signal-to-noise ratio we simply have assumed a power-law spectrum with photon index $\alpha = 2$ for the count rate to flux conversion. The absorption was estimated from the density of neutral Hydrogen in the Galaxy (Dickey & Lockman 1990). Within the large uncertainty of the applied procedure, the energy fluxes of C1 and C2 are found to agree within a factor of two or better with the fluxes given by Shibata et al. (1997) for the power-law model.

Whereas the instruments aboard ASCA and BeppoSAX provide information over a larger energy range, the ROSAT instruments have the better angular resolution and soft response. PSR

Table 1. Properties of the X-ray sources detected by MECS in the neighborhood of PSR B1055–52.

Nr.	Name BX	RA(2000)	DEC(2000)	Rate ^a × 10 ⁻³ cts/s	Nh × 10 ²¹ cm ⁻²	flux ^b × 10 ⁻¹³ erg/s/cm ²
C1	J1058.8-5230	10 58 47.5	-52 30 20	3.2 ± 0.3	2.9	3.3
C2	J1058.2-5233	10 58 10.6	-52 33 49	4.8 ± 0.3	2.9	4.9
C4	J1057.8-5221	10 57 25.2	-52 21 33	2.5 ± 0.2	2.9	2.6

^abackground, dead-time and vignetting corrected, ^bin the 0.5 – 10 keV band pass

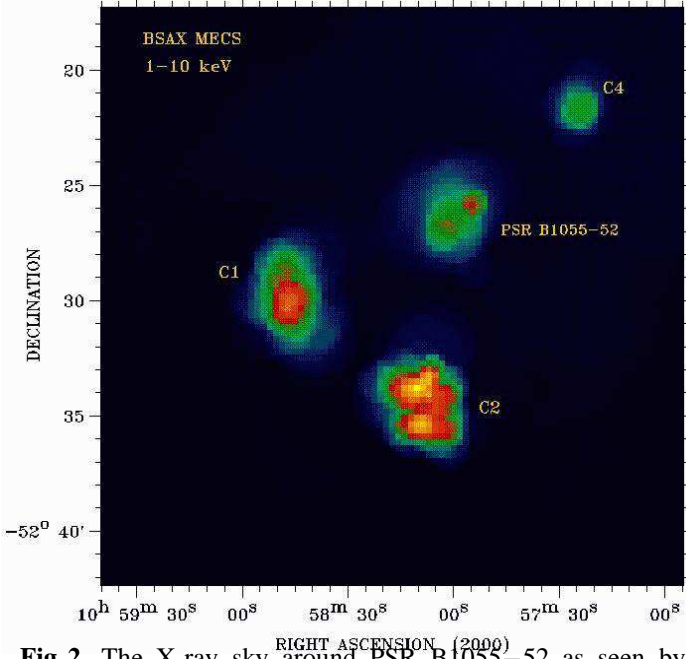


Fig. 2. The X-ray sky around PSR B1055–52 as seen by the MECS aboard BeppoSAX. Only three X-ray sources are detected in the neighborhood of PSR B1055–52. C2 is found to have a fine structure because of few close but spatially not fully resolved sources (see Fig.3, 4). The pulsar itself is very faint beyond 1 keV. Its X-ray emission dominates the soft band below 0.5 keV. A new source C4 which is not seen in the ASCA data is detected in the north-western edge of the image.

B1055–52 was observed with the ROSAT PSPC in January 1992 for an effective exposure time of 15 ksec. Also data from a 9 ksec ROSAT HRI observation are available in the ROSAT archive, but the analysis of these data did not add new information to the PSPC results. Furthermore, the PSPC’s background is much lower than that of the HRI detector, so that the PSPC is the preferable instrument to search for faint and/or diffuse emission.

Using the Extended Scientific Analysis Software *eXsas* (Zimmermann et al. 1994) we have performed a spatial analysis of the pulsar field in the soft (0.1–1.0 keV) and in the hard band (1.0–2.4 keV). 13 sources are detected by the PSPC with a significance $\geq 5\sigma$ at off-axis angles ≤ 20 arcmin, as this field includes the full GIS field of view. The properties of these 13 sources are summarized in Table 2. The PSPC hard band image with the sources encircled is shown in Fig. 3.

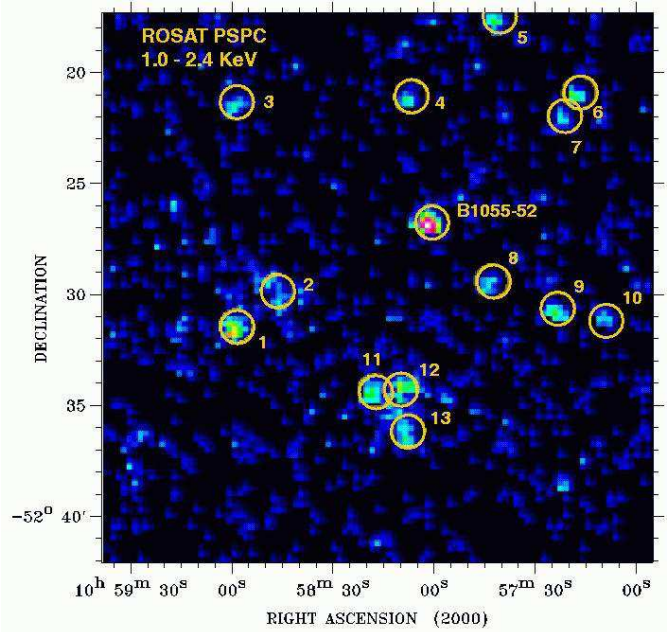


Fig. 3. PSR B1055–52 as seen by the ROSAT PSPC. The image has the same scale as the BeppoSAX MECS image shown in Fig.2. Several faint X-ray sources are detected in the pulsar’s neighborhood. The position of source #2 and #11–13 is in agreement with the location of the X-ray sources C1 and C2 observed by ASCA and MECS (i.e. C2 is resolved into 3 point sources by ROSAT). Source #3 corresponds to “clump C3” of Shibata et al. (1997).

Correlating the position of the sources detected by ROSAT, ASCA and SAX, we have identified the PSPC source #2 as the likely counterpart of the hard X-ray source C1 and the sources #11–13 as the counterparts of C2. Source #3 is found to correspond to the “clump” C3 of Shibata et al. (1997) which is not detected in the MECS data. The PSPC sources #6,7 correspond to source C4 seen in the MECS image (see Fig. 2). The energy fluxes of the PSPC sources are in agreement with what we have measured for their MECS counterparts by adding the fluxes from source #6,7 and #11-13, respectively.

Our analysis has thus shown, that the hard X-ray sources C1 and C2, which are proposed to be caused by the interaction of a pulsar-wind with the interstellar medium, are resolved by the PSPC into single point sources, well separated from the pulsar and unlikely to be associated with it. A result, which is in

Table 2. Properties of the ROSAT PSPC sources, detected in the neighborhood of PSR B1055–52 beyond 1 keV and within an off-axis angle of ≤ 20 arcmin. The given energy range indicates if a source is detected in the full band or beyond 1 keV only. The columns "mag" and "ID" give the estimated R/B-band magnitude and the proposed identification of the optical counterparts found in a 10 arcsec error circle centered on the PSPC position. "S" and "nS" indicate if the sources in the error circle are likely to be identified with a star or with not being a star.

Nr.	Range keV	Name RX	ASCA ID	RA(2000)	DEC(2000)	Rate ^a $\times 10^{-3}$ cts/s	Nh $\times 10^{21}$ cm ⁻²	flux ^b $\times 10^{-13}$ erg/s/cm ²	mag R	mag B	ID
1	0.1-2.4	J1058.9-5231		10 58 58.1	-52 31 36.8	4.6 ± 0.6	2.9	2.3			
2	1.0-2.4	J1058.7-5229	C1	10 58 46.9	-52 29 48.5	2.7 ± 0.4	2.9	2.1	> 22	> 23	
3	1.0-2.4	J1058.9-5221	C3	10 58 57.5	-52 21 23.1	0.8 ± 0.3	2.9	0.6	>22	>23	
4	0.1-2.4	J1058.0-5221		10 58 05.6	-52 21 08.6	1.6 ± 0.4	2.9	1.3			
5	0.1-2.4	J1057.6-5217		10 57 39.4	-52 17 26.8	2.7 ± 0.5	3.3	1.5			
6	0.1-2.4	J1057.2-5220		10 57 15.9	-52 20 55.4	2.1 ± 0.5	3.3	1.1			
7	0.1-2.4	J1057.3-5222		10 57 20.6	-52 22 03.7	1.7 ± 0.5	3.3	1.6			
8	1.0-2.4	J1057.6-5229		10 57 41.8	-52 29 31.7	0.8 ± 0.3	3.3	0.7			
9	0.1-2.4	J1057.3-5230		10 57 22.1	-52 30 48.6	1.8 ± 0.5	3.3	1.0			
10	0.1-2.4	J1057.1-5230		10 57 06.8	-52 30 59.3	2.4 ± 0.5	3.3	1.3			
11	0.1-2.4	J1058.2-5234	C2	10 58 16.4	-52 34 28.1	2.0 ± 0.5	2.9	1.0	13.7	13.9	nS
12	0.1-2.4	J1058.1-5234		10 58 08.0	-52 34 27.1	4.8 ± 0.8	2.9	2.4	21.5	22.2	nS
13	0.1-2.4	J1058.1-5236		10 58 06.6	-52 36 24.1	3.3 ± 0.6	2.9	1.6	18.2	18.0	nS
									14.3	14.1	nS
									18.4	16.2	nS

^abackground, dead-time and vignetting corrected rate in the given range,

^bwithin the 0.5 – 10 keV band pass,

line with a report recently published by Stappers et al. (1999). The authors have performed radio observations of the field around PSR B1055–52 in order to search for diffuse and extended radio counterparts of the putative ASCA pulsar-wind nebulae. Their observations, however, have failed to detect extended plerionic emission associated with PSR B1055–52 (on any spatial scale), but have shown that the position of the ASCA knots C1 and C2 correlate with (unidentified) radio point sources. The radio image of the pulsar field, adopted from Stappers et al. (1999) but with their contour lines removed, is shown in Fig.4. The radio counterparts which we have identified to correspond to the sources C1, C2 and the PSPC sources #1 and #9 are indicated by squares.

A search for possible optical counterparts within a 10 arcsec error circle of the ROSAT sources #2,3 and #11–13 was performed making use of results obtained from the pipeline processing of digitized Schmidt photographic plates, used as input for the generation of the Guide Star Catalog II (McLean et al. 1998). The plates are scanned at 15μ resolution, corresponding to a pixel size of 1 arcsec and the astrometric calibration (accurate to ~ 0.5 arcsec, absolute) has been performed using Tycho/Hipparcos reference stars. Conversion from photographic density to B and R magnitudes has been achieved using inputs from the Guide Star Photometric Catalogue2 (Postman et al. 1998) and are accurate within 0.2 magnitudes. Star/non-star classification is based on the object morphology as characterized by the pipeline. The result of our correlation is included in Table 2. We have found a candidate optical counterpart for

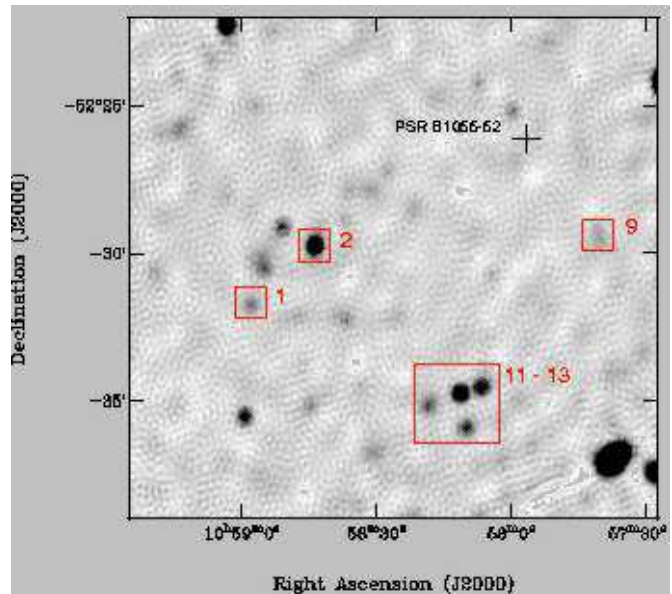


Fig. 4. 1.4 GHz radio image of PSR 1005–52 and its surrounding. The image has been adapted from Stappers et al. (1999). Radio counterparts of the ROSAT detected sources #1,2,9 and # 11-13 are indicated. The sources #2 and #11–13 correspond to the ASCA and MECS detected hard X-ray sources C1 and C2.

each of the sources #2, #11, #13 while for #12 we have found

three objects within the error circle. Although from inspecting the shape of the optical sources we find that they are unlikely to be stars, their final identification is subject of subsequent observations.

2.2. PSR B0656+16

The 384 ms pulsar PSR B0656+14 turns out to be very similar to PSR B1055–52 (see Table 3 of Becker & Trümper 1997). Its inferred pulsar parameters are a spin-down age of 1.1×10^5 yr, a magnetic dipole field $B_{\perp} = 4.7 \times 10^{12}$ G and a spin-down energy $\log \dot{E} = 34.58$ erg/s. The pulsar dispersion measure, based on the Galactic electron density model of Taylor & Cordes (1993), puts PSR B0656+14 at a nominal distance of 760 pc.

X-ray emission from PSR B0656+14 was first seen by the *Einstein* observatory (Cordova et al. 1989). ROSAT Observations detected X-ray pulses at the radio period and identified the soft X-ray emission as radiation from the hot cooling neutron star surface (Finley et al. 1992; Possenti et al. 1997). In addition to the soft X-ray emission, a hard tail component in the X-ray spectrum, indicated from the ROSAT data, was observed by ASCA and identified to be of non-thermal origin (Greiveldinger et al. 1996).

The possible existence in the ASCA data of a ~ 20 arcmin wide putative pulsar-wind nebula around PSR B0656+14 has been communicated by Kawai & Tamura (1996) and by Kawai et al. (1998a, 1998b) but no detailed information about its flux and size is available in the literature. In order to get the best inputs for the search of possible ROSAT counterparts of the hypothetical pulsar wind nebula, we re-analyzed the archival ASCA data of PSR B0656+14. Since the data from the SIS were not found to add further information, we restricted our analysis to the GIS2 and GIS3 data. To optimize the detectors temporal resolution for pulsar timing, the GIS2 and GIS3 were operated in a special PH mode with reduced spatial resolution (raw pixel size 1 arcmin only). Applying the standard screening criteria (no rise-time information was recorded during the observations so that a cleaning for cosmic-ray/particle events could not be performed) we obtained good data from GIS2 and GIS3 for an effective exposure time of 35 807 and 35 806 sec, respectively. Important to note is that in this observation the detector aim-point was placed at the so-called "1 CCD nominal position", which is near the center of S0 chip-1 and S1 chip-3 of the SIS detector. This configuration implies for the GIS data that the pulsar is observed near the optical axis in GIS3 but approximately 5 arcmin off-axis in GIS2 (vice versa for parts of the pulsar surrounding).

Since this configuration results in a different sensitivity map for GIS2 and GIS3² and both detectors have a different energy response, we have decided to analyse the images from GIS2 and GIS3 separately.

In order to visually enhance faint (and extended) structures in the noise-dominated GIS data we have processed the extracted images with an adaptive kernel smoothing (Ebeling et al. 1999). The advantage of this kind of image processing compared to a simple Gaussian smoothing (which can produce strong artifacts easily miss-interpreted as pulsar-wind nebula) is that noise is suppressed very efficiently while at the same time real structure is preserved on all scales.

Fig. 5a shows the GIS2 image, with the pulsar observed off-axis. Two faint point sources C1 and C2 are clearly visible south of the pulsar. The brighter source C1 is closest to the detector optical axis where the instrument is most sensitive. There is no indication for the existence of a ~ 20 arcmin wide clumpy pulsar-wind nebula in this data. Indeed, the putative pulsar-wind nebula, which Kawai & Tamura (1996) found to have a shape like the "trunk of an elephant", actually consists of two point sources. This is confirmed by the GIS3 image shown in Fig.5b, where the pulsar is observed on-axis and the two faint sources C1 and C2 are about 5 arcmin off-axis. At this position, the sensitivity and spatial resolution of the detector are noticeably lower than on-axis, so that the sources C1 and C2 are only barely visible/resolved. A third source (C3) is also visible in the GIS3 image, north-west of the pulsar. Due to their low signal-to-noise ratios, no spectral analysis is possible on the sources C1–C3.

Since BeppoSAX observed PSR B0656+14 only in 1999 January and the data are not yet available to us, we concentrate our search for soft X-ray counterparts of C1–C3 using the ROSAT data only. PSR B0656+14 was observed by ROSAT with both the PSPC and HRI detectors in March 1991 and 1992 for an effective exposure time of 16 ksec and 10 ksec, respectively. Spatial analysis of the PSPC field, restricted to an off-axis angle ≤ 20 arcmin, detected 15 sources, at a significance $\geq 5\sigma$. Apart from the pulsar itself, all sources are rather faint with typical counting rates of $(3 - 8) \times 10^{-3}$ cts/s (see Table 3 for a summary of their properties). A spectral analysis is therefore precluded by the low number of detected counts. The PSPC hard band image, showing the central inner region of the PSPC detector with the detected sources encircled, is shown in Fig. 6.

After a spatial correlation between the PSPC and the ASCA image we identified the ROSAT sources #14,15 and #3 as the likely counterparts of the clumps C1–C3. In order to improve the positions of the PSPC sources (accurate within $\simeq 10$ arcsec, including systematic errors like pointing inaccuracies of the satellite), we have analyzed archival HRI data. However, due to the 3-5 times lower sensitivity of the HRI with respect to the PSPC and the shorter exposure, we found that only source #15 is marginally detected, with a position (RA=06:59:38.26 and DEC= +14:00:30.8) in agreement with the PSPC one (see Table 3). Again, a search for optical counterparts within 10 arc-

² Both instruments are most sensitive at the optical axis and noticeable less sensitive 5 arcmin away from it.

sec error circles of the ROSAT sources #14,15 and #3 (i.e. C1–C3) was performed using digitized POSS-II B and R plates. The result of our correlation is also included in Table 3. For each of the interesting sources, we have found candidate optical counterparts. Although the nature of the ROSAT sources #14,15 and #3 has still to be assessed, our analysis suggests that they are the counterparts of the emission clumps observed by ASCA and that they are background objects unrelated to the pulsar.

In the radio band a search for a pulsar-wind nebula surrounding PSR B0656+14 was originally performed by Cordova et al. (1989) using the VLA. The authors reported on a candidate source about 1.2 – 3.3 arcmin away from the pulsar (Fig. 7), which appeared slightly extended and about 40 – 50% linear polarized. This was taken as a clear sign that the radio emission of this source is due to synchrotron radiation (as expected for a plerion). Our analysis shows that the extended radio source of Cordova et al. (1989) coincides with the position of the hard PSPC source #11, although undetected by the Einstein Observatory. Whether this radio/X-ray source is really related to the pulsar or whether it is an unrelated background object remains to be subject to further studies.

2.3. Geminga

The Geminga pulsar was first noticed as a strong gamma-ray source (Fichtel et al. 1975) and only recently found to be a rotation-powered pulsar (Halpern & Holt 1992; Becker et al. 1993). It has a spin-down age of 3.4×10^5 yr, an inferred magnetic dipole component of $B_{\perp} = 1.6 \times 10^{12}$ G and a spin-down energy of $\log \dot{E} = 34.51$ erg/s (Bertsch et

al. 1992). Its distance of 159_{-34}^{+59} pc was determined from optical parallax measurements using the HST (Caraveo et al. 1996).

X-ray emission from Geminga was first detected by the *Einstein* observatory (Bignami et al. 1983). However, as for PSR B1055–52, the sensitivity of ROSAT was required to detect its X-ray pulses and to identify its soft X-ray emission as radiation from the hot cooling neutron star surface (Halpern & Holt 1992). A harder spectral component, first interpreted as thermal emission from a hot polar-cap, was later identified with ASCA to be of non-thermal (magnetospheric) origin (Halpern & Wang 1997; see also Becker & Trümper 1997 and the discussion therein). The possible existence of a ~ 20 arcmin wide pulsar-wind nebula around Geminga was first reported by Kawai et al. (1998a, 1998b).

In order to check the significance of this putative pulsar-wind nebula and to probe the pulsar surrounding in more detail we reanalyzed the archival ASCA data of Geminga. The pulsar was observed by ASCA in 1994, March 28 for an exposure of about 71 ksec. The observation was performed with an instrument setting similar to that used for the observation of PSR B0656+14 (i.e. 1×1 arcmin pixel size for the GIS detectors, source at the 1-CCD nominal position). Unlike for PSR B0656+14, rise-time information was recorded during the observation so that we could apply the standard screening criteria including a data cleaning for cosmic- and particle events. The data of GIS2 and GIS3 were analyzed separately for the known reasons (see Sect. 2.2). The GIS2 and GIS3 images, smoothed with an adaptive top-hat kernel (Ebeling et al. 1999), are shown in Fig. 8.

In the GIS2 image (Fig. 8a) the pulsar is observed about 5 arcmin off-axis. Few faint point sources (C1–C3) are visible to the optical axis where the detector’s sensitivity and spatial resolution is higher. Three more sources (C4–C6) are visible to the west of the pulsar. The column “mag” and “ID” in the table below give the estimated B-band magnitude and the proposed identification of the optical counterparts found in a 10 arcsec radius centered on the PSPC position. “nS” indicate that the source in the error circle is likely to be identified with not being a star.

Table 3. Properties of the ROSAT PSPC sources, detected beyond 1 kpc within a region of ~ 20 arcmin around PSR B0656+14. The given energy range indicates if a source is detected in the full band or beyond the pulsar. The column “mag” and “ID” give the estimated B-band magnitude and the proposed identification of the optical counterparts found in a 10 arcsec radius centered on the PSPC position. “nS” indicate that the source in the error circle is likely to be identified with not being a star.

Nr.	Range keV	Name RX	ASCA ID	RA(2000)	DEC(2000)	Rate ^a $\times 10^{-3}$ cts/s	mag	ID
1	0.1–2.4	J0700.5+1407		07 00 32.6	+14 07 17.6	3.22 ± 0.60	19.4	nS
2	0.1–2.4	J0700.7+1422		07 00 42.8	+14 22 03.7	7.02 ± 0.87	19.4	nS
3	1.0–2.4	J0700.2+1421	C3	07 00 15.0	+14 21 03.7	5.93 ± 0.21	22.9	nS
4	0.1–2.4	J0700.1+1422		07 00 09.5	+14 22 11.9	4.02 ± 0.62	22.9	nS
5	0.1–2.4	J0700.1+1429		07 00 08.1	+14 29 27.9	1.10 ± 0.13	22.9	nS
6	0.1–2.4	J0659.7+1421		06 59 45.8	+14 21 54.7	1.13 ± 0.52	22.9	nS
7	1.0–2.4	J0659.4+1415		06 59 29.7	+14 15 57.5	5.59 ± 0.36	22.9	nS
8	0.1–2.4	J0659.3+1416		06 59 19.6	+14 16 06.1	2.26 ± 0.49	22.9	nS
9	0.1–2.4	PSR B0656+14		06 59 48.1	+14 14 25.4	1897.24 ± 10.0	22.9	nS
10	0.1–2.4	J0659.9+1412		06 59 56.5	+14 12 25.7	6.32 ± 0.80	22.9	nS
11	1.0–2.4	J0659.8+1412		06 59 48.0	+14 12 50.0	0.83 ± 0.25	22.9	nS
12	0.1–2.4	J0659.1+1411		06 59 11.8	+14 11 18.1	4.46 ± 0.66	22.9	nS
13	0.1–2.4	J0658.7+1411		06 58 47.8	+14 11 52.4	2.93 ± 0.63	22.9	nS
14	0.1–2.4	J0659.4+1404	C1	06 59 25.4	+14 04 44.2	3.70 ± 0.62	20.8	nS
15	0.1–2.4	J0659.6+1400	C2	06 59 37.7	+14 00 18.9	1.18 ± 0.93	20.8	nS

^a background, dead-time and vignetting corrected rate in the given energy range.

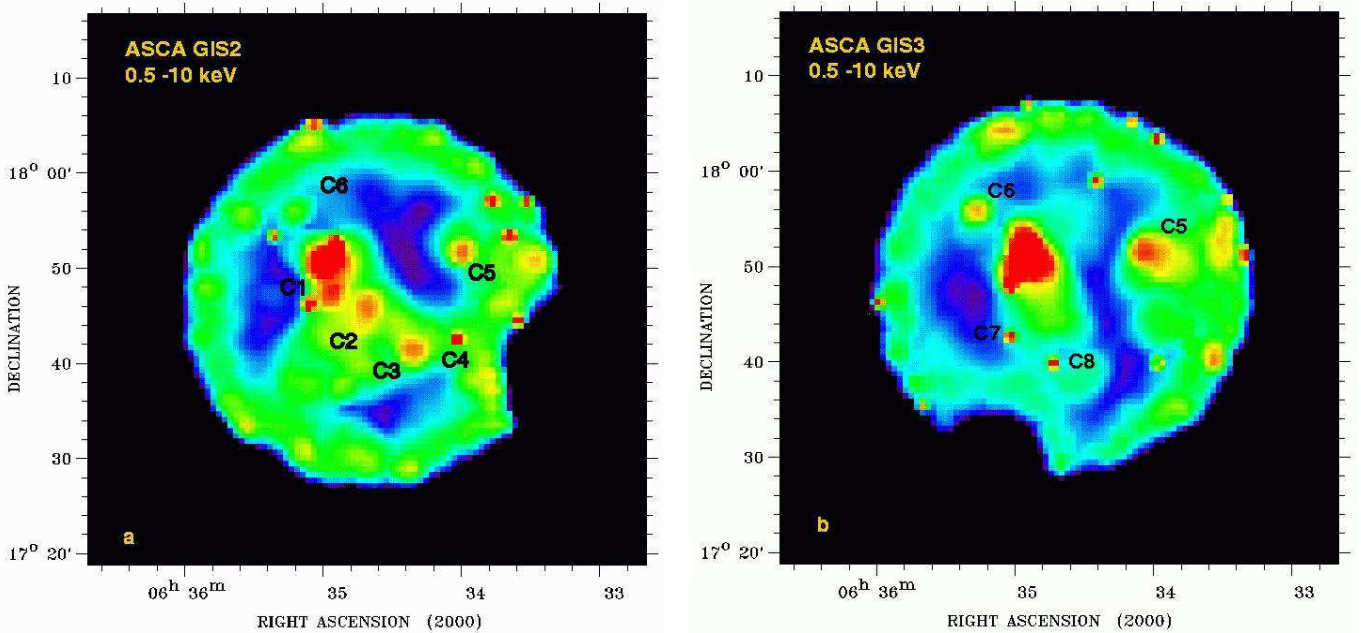


Fig. 8. a,b Geminga and its surrounding as seen with the ASCA GIS2 (top) and GIS3 (bottom). Shown is the GIS’s central ~ 44 arcmin field of view (images are not vignetting corrected). The pulsar is the brightest source in the field. Few faint point sources (labeled C1–C8) are detected in the neighborhood of Geminga.

field we applied a Maximum-likelihood source detection in the soft (0.1–1.0 keV) and in the hard band (1.0–2.4 keV) using *eXsas*. In total, 73 sources are detected with a significance of more than 5σ in the PSPC full field of view. This implies a density of soft X-ray sources which is about a factor of two higher than observed in the neighborhood of PSR 0656+14 and PSR 1055–52. The reason for that is that Geminga is located close to the edge of the Monogem ring (Fig. 10), a ~ 20 degree wide object which is believed to be an old and close by supernova remnant (see for example Plucinsky et al. 1996). Actually, a large fraction of the detected sources is found to be diffuse and fuzzy emission of a small part of the Monogem ring that dominates the southern part of the detector field (see Fig. 9). The emission from the Monogem ring is very soft so that in the hard band beyond 1 keV only 36 sources are detected in the full field of view. 23 of these sources are located at off-axis angles ≤ 20 arcmin, matching the GIS full field of view. Their properties are summarized in Table 4.

Inspecting the HRI data only Geminga and the PSPC source #2 are detected. This source was already noticed in the Einstein data as well as in a short ROSAT HRI observation (Becker et al. 1993). Its improved HRI position, extracted after correcting the data for a 3 arcsec attitude error recently found to be present in all HRI pointings, is RA=06:34:06.6, DEC=17:59:53, in agreement with its PSPC position. We further checked the source extent of Geminga and found it to be in agreement with the HRI point-spread function.

After a spatial correlation of the ROSAT and ASCA frames, we have identified the PSPC sources #18,17,15,13,11,9,20

and #21 as the likely counterparts of the hard X-ray clumps C1–C8. The faint diffuse and bridge-like emission seen in the GIS2 image south of the sources C1–C3 is possibly due to the unresolved emission of the sources #19–23.

A search for optical counterparts within a 10 arcsec error circle of the sources C1–C8 was performed using the digitized POSS-II plates. Five of them were found to have optical candidate counterparts (Table 4). A correlation with the 1.4 GHz NRAO/VLA Sky Survey (Condon et al. 1998) revealed radio counterparts for the sources #4 and #9 (C6), using a search radius of 15 arcsec.

3. Summary and discussion

Based on ASCA observations of rotation-powered pulsars Kawai & Tamura (1996), Shibata et al. (1997) and Kawai et al. (1998a, 1998b) have reported on the possible existence of huge, 10–20 arcmin wide X-ray bright nebulae around most of the ASCA detected pulsars. The existence of these nebulae was explained by an interaction of a pulsar-wind outflow with the surrounding interstellar matter. In particular, the X-ray luminosity of these nebulae was found to correlate with the pulsar spin-down energy \dot{E} (Kawai et al. 1998b). Interpreted as a universal phenomenon, Shibata (1998) used these pulsar-wind nebulae as a calorimeter to constrain parameters of the pulsar wind and the confining pressure of the ambient medium.

In order to assess the reality of these nebulae, we have performed a careful study of the fields around the three musketeers PSR B1055–52, B0656+14, and Geminga, based on a com-

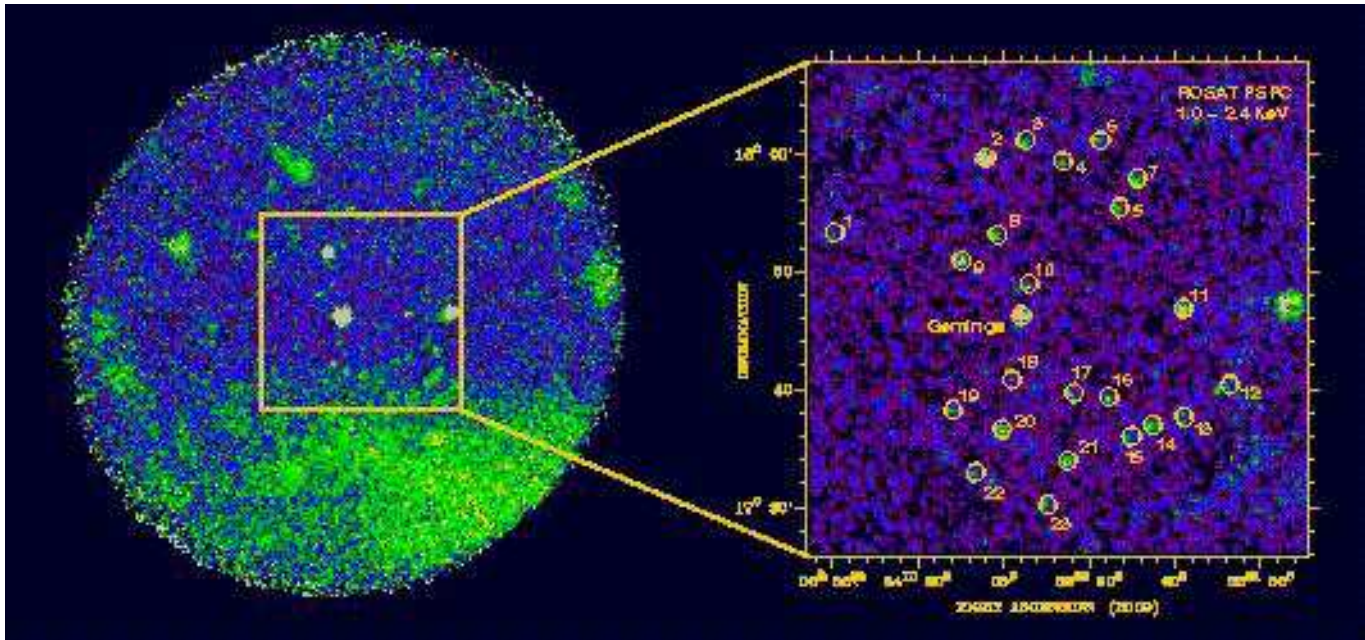


Fig. 9. The Geminga field as seen by the ROSAT PSPC in the energy range 0.1-2.4 keV. Shown is the PSPC's 2° full field of view (exposure and vignetting corrected). The pulsar is the bright central point source. The diffuse and fuzzy emission which dominates the southern part of the detector field belongs to the Monogem ring (Fig.10). The insert marks the inner region of the PSPC detector. 23 X-ray sources are detected beyond 1 keV in a 40×40 arcmin square centered on the pulsar. Their positions are indicated in the hard band image shown on the right. The positions of the PSPC sources #18,17,15,13,11,9,20 and #21 are in agreement with the location of the X-ray clumps C1–C8 detected in the ASCA GIS data.

bin analysis using archival ASCA, BeppoSAX and ROSAT data.

Based on these data we could not establish the reality of the 10 – 20 arcmin wide X-ray bright and clumpy pulsar-wind nebula around the three musketeers. In all cases faint, point-like, X-ray sources were found and clearly resolved by the ROSAT PSPC, well separated from the pulsar and coincident with the knots reported by Shibata et al. (1997) and Kawai et al. (1998a, 1998b). On a larger scale, our analysis showed that the spatial distribution of these sources follows quite well the shape of the putative X-ray nebulae. For most of them we have found candidate optical counterparts in digitized photographic plates and for the sources around PSR B1055–52 we also identified likely radio counterparts in data taken by Stappers et al. (1999). NVSS radio data (Condon et al. 1998) were used to search for radio counterparts of the X-ray sources around Geminga and PSR 0656+14.

Although the visual appearance of weak emission patterns can sensitively depend on details of the image construction method, the existence of optical and radio counterparts for many of these X-ray sources strongly favors their interpretation as isolated point sources. We therefore conclude that the apparent clumpy extended emission observed in ASCA data was probably caused by the unresolved contribution of point sources located in the vicinity of the pulsars, enhanced by data-analysis artifacts like incomplete source subtraction, background modeling and Gaussian smoothing.

We remind that the three musketeers are located close to the galactic plane, i.e. in crowded regions. Indeed, our analysis has shown that, on average, about 20 hard X-ray sources (e.g. identified beyond 1 keV) are detected with the PSPC in a region which corresponds to the GIS full field of view. Even if most of these sources are not detected by the GIS, they contribute to the background emission which – by the lack of spectral information – is difficult to model.

These results are in line with similar findings recently reported by Brinkmann et al. (1999) and Pivovarov et al. (1999) who could not confirm the existence of the putative pulsar-wind nebula surrounding PSR B1610–50 and PSR B1046–58.

Of course, the sensitivity of our pulsar-wind nebulae search is background limited. However, given the lack of models predicting the extent or the surface brightness of the nebula as a function of the pulsars' parameters we restrain from giving explicit upper limits as this would require *ad hoc* assumptions on a nebula size and properties. The different behavior observed for the plerions around the Crab-, PSR 1509-58 and Vela support this view. While for the Crab-nebula ($d=2$ kpc, extent $\sim 2'$) the emission efficiency in terms of the pulsar spin-down energy is $\sim 5\%$ in the ROSAT band, it is only $\sim 1\%$ for the nebula around PSR 1509-58 ($d=4.9$ kpc, extent $7' \times 9'$) and $\sim 0.04\%$ for the Vela-nebula ($d=0.5$ kpc, extent $2'$) (Becker & Trümper 1997). Finally, we note that the results of our analysis does not argue against the presence of compact synchrotron nebulae on smaller scales. However, the ROSAT HRI data available for all of the investigated sources restrict their extension to less than

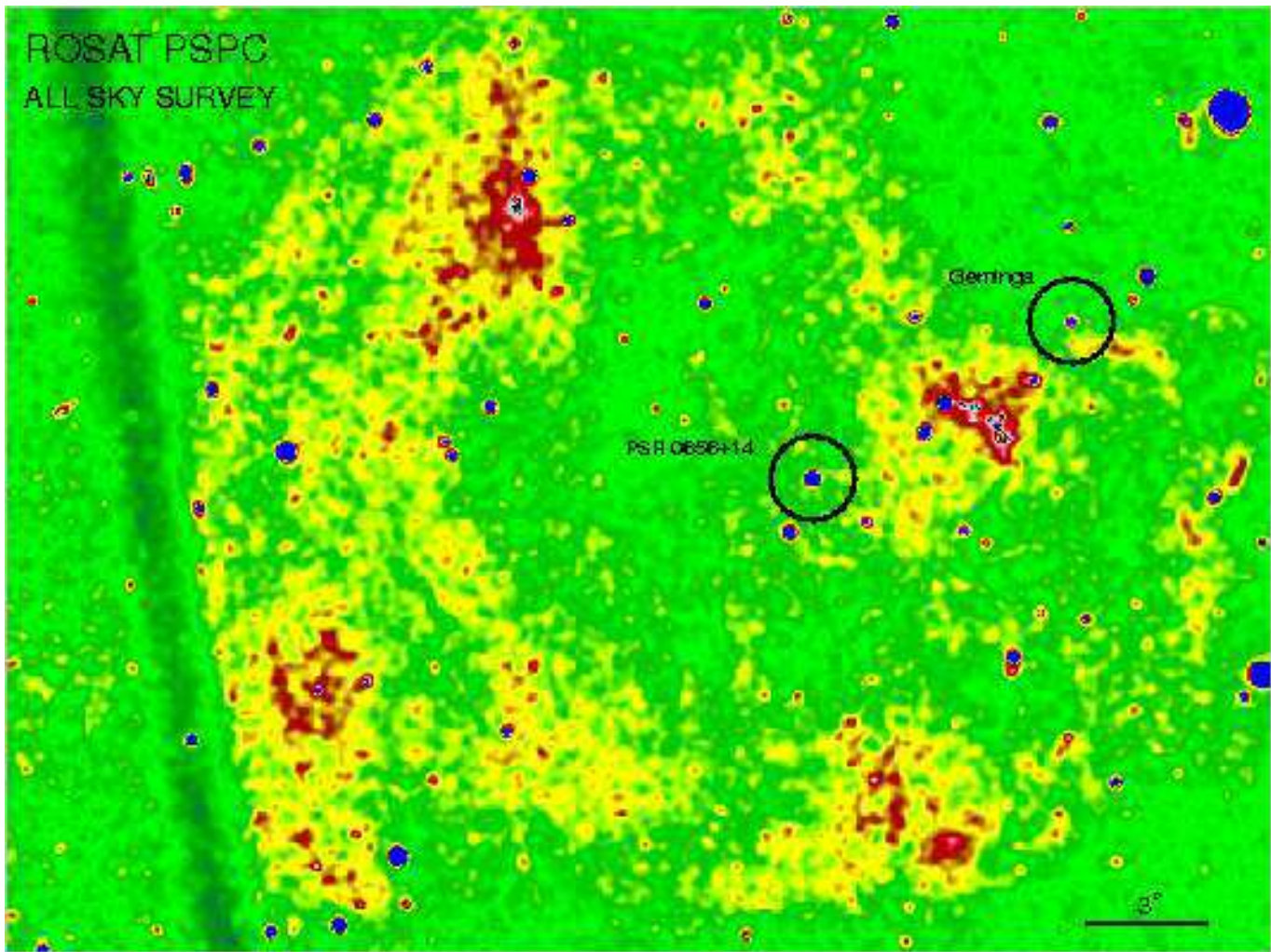


Fig. 10. The $\sim 20^\circ$ wide Monogem ring as observed in the ROSAT all-sky survey. The PSPC FOV during the pointed observations of Geminga and PSR 0656+14 are indicated. The image demonstrates that both pulsars are located in crowded regions with fuzzy background emission, difficult to disentangle with ASCA's spatial resolution of ~ 3 arcmin.

~ 10 arcsec. Providing a resolving power of 1 arcsec it will be interesting to see what information Chandra will add to this issue.

Acknowledgements. The ROSAT project is supported by the Bundesministerium für Bildung, Wissenschaft, Forschung und Technologie (BMBW) and the Max-Planck-Society (MPG). We thank our colleagues from the MPE ROSAT group for their support. WB & WB thank the Cosmic Radiation Laboratory for hospitality where part of the research was done in the framework of the RIKEN-MPE exchange program. WB is grateful to G. Cusumano from IFCAI/CNR for support during the reduction of BeppoSAX data. On behalf of the GSC2 Project collaboration, RM wants to dedicate his contribution to the present paper to the memory of Barry Lasker. The Guide Star Catalogue-II is produced by the Space Telescope Science Institute, in collaboration with the Osservatorio Astronomico di Torino. Additional support is provided by the Association of Universities for Research in Astronomy, the Italian Council for Research in Astronomy, European Southern Observatory, Space telescope European Coordinating facility, the International GEMINI project and the European Space Agency Astrophysics Division.

References

- Becker W., Trümper J., 1997, *A&A* 326, 682
 Becker W., Brazier K.T.S., Trümper J., 1993, *A&A* 273, 421
 Bertsch D.L., Fichtel C.E., Hartman R.C., et al., 1992, *Nat* 357, 306
 Bignami G.F., Caraveo P.A., Lamb R.C., 1983, *ApJ* 272, L9
 Boyd P.T., van Citters G.W., Dolan J.F., et al., 1995, *ApJ* 448, 365
 Brinkmann W., Ögelman H., 1987, *A&A* 182, 71
 Brinkmann W., Kawai N., Scheingraber H., Tamura K, Becker W., 1999, *A&A* 346, 599
 Caraveo P.A., Bignami G.F., Mignani R., Taff L., 1996, *ApJ* 461, L91
 Cheng A.F., Helfand D.J., 1983, *ApJ* 271, 271
 Condon J.J., Cotton W.D., Greisen E.W. et al., 1998, *AJ* 115, 1693
 Cordova F.A., Hjellming R.M., Mason K.O., Middleditch J., 1989, *ApJ* 345, 451
 Dickey J.M., Lockman F.J., 1990, *ARA&A* 28, 215
 Ebeling H., White D.A., Rangarajan F.V.N., 1999, submitted to *MNRAS*
 Fichtel C.E., Hartman R.C., Kniffen D.A., et al., 1975, *ApJ* 198, 163
 Finley J.P., Ögelman H., Kiziloglu Ü., 1992, *ApJ* 394, L21
 Greiveldinger C. et al, 1996, *ApJ* 465, L35

Table 4. Properties of the ROSAT PSPC sources detected within a region of ≤ 20 arcmin around Geminga.

Nr.	Range keV	Name RX	ASCA ID	RA(2000)	DEC(2000)	Rate ^a $\times 10^{-3}$ cts/s	mag B	mag R	ID
1	1.0-2.4	J0635.0+1753		06 35 00.52	17 53 16.6	0.72 \pm 0.17			
2	0.1-2.4	J0634.1+1759		06 34 06.92	17 59 45.9	34.47 \pm 0.88			
3	0.1-2.4	J0633.8+1801		06 33 53.16	18 01 13.9	2.08 \pm 0.32			
4	1.0-2.4	J0633.6+1759		06 33 39.45	17 59 28.9	0.45 \pm 0.11			
5	0.1-2.4	J0633.3+1755		06 33 18.96	17 55 22.5	0.94 \pm 0.21			
6	0.1-2.4	J0633.4+1801		06 33 26.04	18 01 07.5	1.37 \pm 0.29			
7	0.1-2.4	J0633.2+1757		06 33 12.52	17 57 54.1	1.69 \pm 0.29			
8	0.1-2.4	J0634.0+1753		06 34 02.89	17 53 05.3	1.10 \pm 0.20			
9	0.1-2.4	J0634.2+1750	C6	06 34 15.30	17 50 58.9	2.46 \pm 0.26	>22.5	>20.8	
10	0.1-2.4	J0633.8+1748		06 33 51.47	17 48 44.6	1.67 \pm 0.24			
Gem	0.1-2.4	J0633.9+1746		06 33 54.33	17 46 11.9	504.24 \pm 3.10			
11	0.1-2.4	J0632.9+1746	C5	06 32 56.35	17 46 43.9	3.41 \pm 0.32	>22.5	> 20.8	
12	1.0-2.4	J0632.6+1740		06 32 39.64	17 40 07.7	1.01 \pm 0.20			
13	0.1-2.4	J0632.9+1737	C4	06 32 55.97	17 37 34.1	1.58 \pm 0.32	18.9	18.3	nS
14	0.1-2.4	J0633.1+1736		06 33 06.50	17 36 41.8	1.43 \pm 0.27			
15	1.0-2.4	J0633.2+1735	C3	06 33 14.99	17 35 41.4	0.94 \pm 0.18	>22.5	>20.8	
16	1.0-2.4	J0633.3+1739		06 33 22.99	17 39 05.1	0.61 \pm 0.12			
17	1.0-2.4	J0633.5+1739	C2	06 33 35.53	17 39 27.2	0.33 \pm 0.09	14.3	12.7	?
18	0.1-2.4	J0633.9+1740	C1	06 33 56.89	17 40 46.0	1.26 \pm 0.22	16.9	17.5	?
19	1.0-2.4	J0634.3+1737		06 34 18.52	17 37 58.2	0.33 \pm 0.09			
20	0.1-2.4	J0634.0+1736		06 34 01.47	17 36 15.7	2.45 \pm 0.30			
21	0.1-2.4	J0633.6+1733	C7	06 33 37.41	17 33 41.4	1.75 \pm 0.26	18.4	21.0	nS
22	0.1-2.4	J0634.2+1732	C8	06 34 10.53	17 32 30.0	1.23 \pm 0.25	>22.5	> 20.8	
23	1.0-2.4	J0633.7+1729		06 33 44.78	17 29 48.8	0.55 \pm 0.13			

^abackground, dead-time and vignetting corrected rate in the given energy range.

Halpern J.P., Holt S.S., 1992, Nat 357, 222

Halpern J.P., Wang F.Y.-H., 1997, ApJ 477, 905

Kaspi V.M. Johnston S., Bell J., et al., 1994 ApJ 423, L43

Kawai N., Tamura K., 1996, in *Pulsars: Problems and Progress. IAU Colloquium 160*, eds. S.Johnston, M.A. Walker, M. Bailes, A.S.P. Conf. Ser., Vol.105, p367

Kawai N., Tamura K., Saito Y., 1998a, Adv. Space Res. Vol.21, No.1/2, pp203

Kawai N., Tamura K., Shibata S., 1998b in *Neutron Stars and Pulsars: Thirty years after the discovery*, eds. N. Shibasaki, N. Kawai, S. Shibata, T. Kifune, Universal Academy Press, Tokyo, p449

Lyne A. G, Pritchard R. S, Graham-Smith F., Camilo F., 1996, Nat 381, 497

Lyne A. G, Pritchard R. S, Smith F. G., 1988, MNRAS 233, 667

McLean B., Hawkins C., Spagna A., et al, 1998 in *New Horizons from Multi-Wavelength Sky Surveys*, Proceedings of the 179th Symposium of the International Astronomical Union, Kluwer Academic Publishers, eds. B.J. McLean, D.A. Golombek, J.J.E. Hayes, H.E. Payne, p. 431.

Ögelman H., Finley J.P., 1993, ApJ 413, L31

Pacini F., 1967, Nat 221, 567

Pivovarov M.J., Kaspi V.M., Gotthelf E.V., 1999, submitted to ApJ

Plucinsky P.P., Snowden S.L., Aschenbach B., et al., 1996, ApJ 463, 224

Possenti A., Mereghetti S., Colpi A., 1997, A&A 313, 565

Postman M., Bucciarelli B., Sturch C., et al., 1998 in *New Horizons from Multi-Wavelength Sky Surveys*, Proceedings of the 179th Symposium of the International Astronomical Union,

Kluwer Academic Publishers, eds B.J. McLean, D.A. Golombek, J.J.E. Hayes, H. E. Payne, p379.

Shibata S., 1998, in *Pacific Rim Conference on Stellar Astrophysics*, eds. K.L. Chan, K.S. Cheng, H.P. Singh, ASP Conference Series, Vol 138, p299

Shibata S., Sugawara, T., Gunji, S., et al., 1997, ApJ 483, 843.

Stappers, B.W., Gaensler, B.M., Johnston S., 1999, MNRAS, in press

Taylor, J.H., Cordes, J.M., 1993, ApJ 411, 674

Wang F.Y.-H., Ruderman M., Halpern J.P., Zhu T. , 1998, ApJ 498, 373

Zimmermann H.U., Becker W., Belloni T., et al., 1994, MPE-Report 244

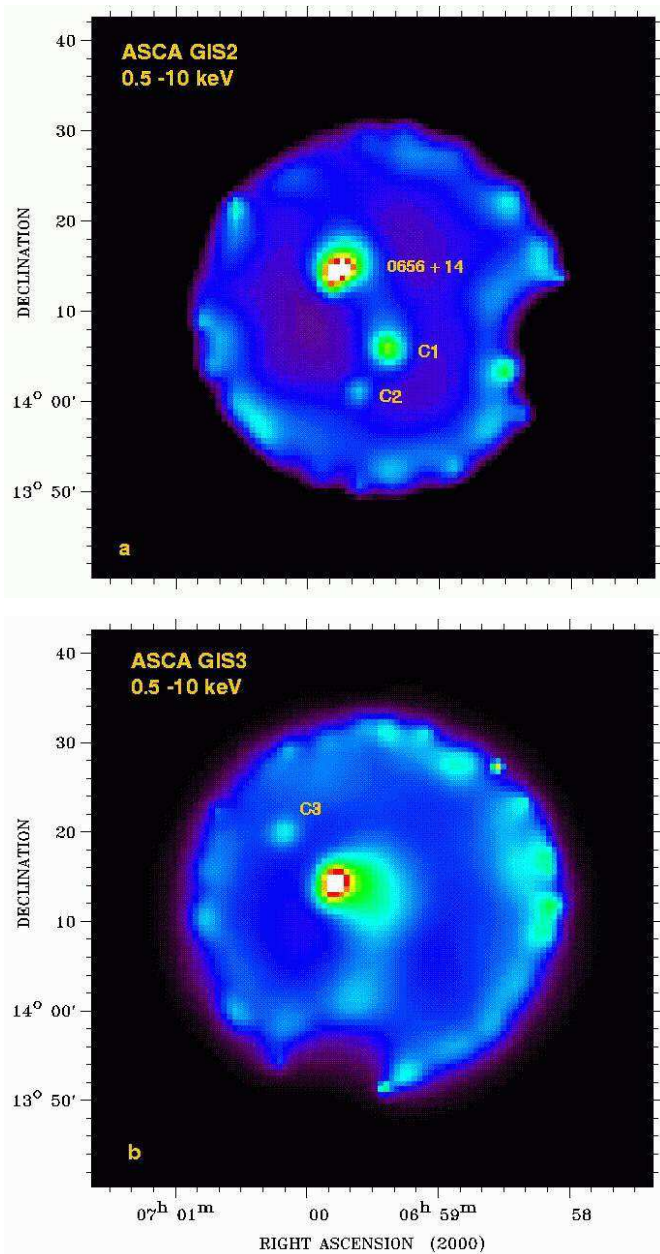


Fig. 5. a,b PSR B0656+14 and its surrounding as seen with the ASCA GIS2 (top) and GIS3 (bottom). Shown is the GIS central ~ 44 arcmin field of view (images are not vignetting corrected). The pulsar is the brightest source in the field. Two faint but hard sources C1 and C2 show up close to the GIS2 optical axis. These sources are observed off-axis by the GIS3 and are barely visible. A third faint point source C3 shows up in the north-western direction from the pulsar. In both images there is no indication for a pulsar-wind nebula. The apparently brighter emission at the edges of the detector fields appears because most non X-ray background events in the GIS are registered close to the detector walls.

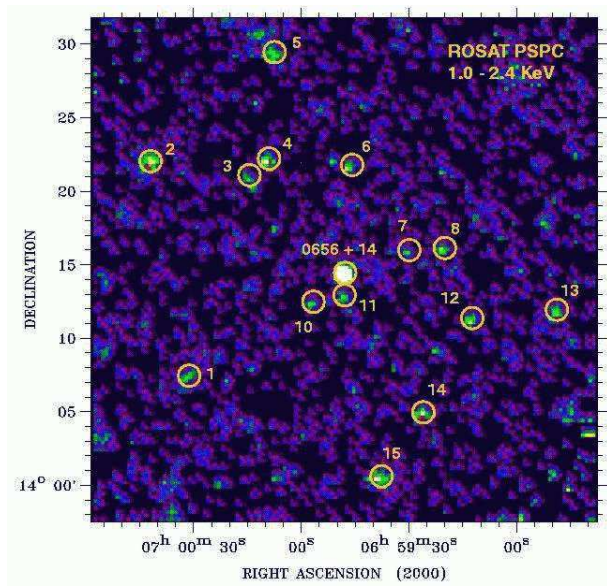


Fig. 6. The PSR B0656+14 field as seen by the ROSAT PSPC. The pulsar is the bright central point source. The position of source #14,15 and #3 is in agreement with the location of the X-ray sources C1–C3 observed by the ASCA GIS. The position of source #11 corresponds to a slightly extended radio source discussed in Cordova et al. (1989).

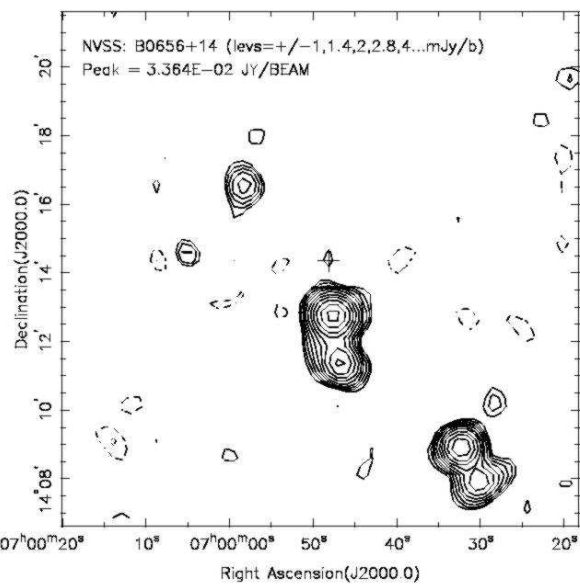


Fig. 7. The PSR B0656+14 field as seen in the NVSS (Condon et al. 1998). The location of the pulsar is marked by a cross. The close by radio source ~ 1.5 arcmin south of the pulsar is observed to be 40-50% polarized (Cordova et al. 1989) and shows up in our correlation to be the radio counterpart of the PSPC source #11.